Tetranuclear Mixed-Metal $M^{II}_2Cu^{II}_2$ Complexes Derived from a Phenol-Based Macrocyclic Ligand Having Two $N(amine)_2O_2$ and Two $N(imine)_2O_2$ Metal-Binding Sites

Yuki Nakamura, Masami Yonemura, Keisuke Arimura, Naoki Usuki, Masaaki Ohba, and Hisashi Ōkawa*

Department of Chemistry, Faculty of Science, Kyushu University, Hakozaki, Higashiku, Fukuoka 812-8581, Japan

Received October 20, 2000

The reaction of *N,N*′-dimethyl-*N,N*′-ethylenebis(5-bromo-3-formyl-2-hydroxybenzylaminato)copper(II) with ethylenediamine in aqueous DMF with excess perchloric acid resulted in the [2:2] cyclic condensation of the constituents, providing the dinuclear Cu^{II} complex $[Cu_2(H_2R)](ClO_4)_2$. It crystallizes in the monoclinic space group $P2_1/c$, with $a = 19.603(3)$ Å, $b = 13.370(2)$ Å, $c = 21.072(3)$ Å, $\beta = 98.87(1)°$, $V = 5456(1)$ Å^3, and $Z = 4$. The ligand R^{4-} has two $N(amine)_2O_2$ and two $N(imine)_2O_2$ metal-binding sites sharing two phenolic oxygens, and $[Cu_2(H_2R)](ClO_4)_2$ has the two Cu^{II} ions in the $N(imine)_2O_2$ sites and two protons in the $N(amine)_2O_2$ sites. $[Cu_2(H_2R)](ClO_4)_2$ was converted by neutralization into $[Cu_2(R)]$, from which mixed-metal $Cu^{II}_2M^{II}_2$ complexes $[Cu_2M_2(R)Cl_4]$ ($M = Co^{II}$, Ni^{II}, Zn^{II}) were derived. $[Cu_2Co_2(R)Cl_4]\cdot 2CHCl_3\cdot H_2O$ crystallizes in the monoclinic space group $C2/c$, with $a = 32.514(3)$ Å, $b = 12.246(3)$ Å, $c = 19.827(2)$ Å, $\beta = 126.082(1)°$, $V = 6380(1)$ Å^3, and $Z = 4$. $[Cu_2Zn_2(R)Cl_4]\cdot 2CHCl_3\cdot H_2O$ crystallizes in the monoclinic space group $C2/c$, with $a = 32.53(1)$ Å, $b = 12.242(2)$ Å, $c = 19.729(9)$ Å, $\beta = 126.03(3)°$, $V = 6354(4)$ Å^3, and $Z = 4$. The two complexes are isotructural and have a dimer-of-dimers structure with two separated $Cu^{II}M^{II}$ units. In each dinuclear unit, the Cu^{II} is bound to the $N(imine)_2O_2$ site and the M^{II} is bonded to a phenolic oxygen and two nitrogens of the $N(amine)_2O_2$ site. The Cu^{II} and M^{II} ions are bridged by a phenolic oxygen and an exogenous chloride ion. The $Cu^{II}_2Ni^{II}_2$ complex has a defect double-cubane structure. Cryomagnetic studies for the $Cu^{II}_2Co^{II}_2$ complex indicate an antiferromagnetic spin-exchange interaction within each dinuclear $Cu^{II}Co^{II}$ unit ($J = -9.5$ cm^{-1} based on $H = -2JS_{Cu}S_{Co}$). The $Cu^{II}_2Ni^{II}_2$ complex shows a weak antiferromagnetic interaction between the adjacent Cu^{II} and Ni^{II} ions (-3.5 cm^{-1}) and a weak ferromagnetic interaction between the two Ni^{II} ions ($+2.0$ cm^{-1}).

Introduction

Heteronuclear metal complexes are of current interest due to their unique physicochemical properties and functions arising from interaction or interplay of dissimilar metal ions in close proximity.[1,2] Dinucleating compartmental ligands having dissimilar metal-binding sites have been developed for providing discrete heterodinuclear metal complexes.[3] On the other hand, little attention has been paid to compartmental ligands that can provide mixed-metal complexes of higher nuclearity. Previously, we reported a phenol-based tetranucleating compartmental ligand that has two $N(amine)_2O_2$ and two $N(imine)_2O_2$ metal-binding sites (hereafter called aminic and iminic sites) in an alternate fashion sharing the phenolic oxygens in a macrocyclic framework[4] (see Scheme 1; abbreviated as R^{4-}). It was obtained as a dinuclear Cu^{II} complex $[Cu_2(R)]$ in a low yield in the cyclization of *N,N*′-dimethyl-*N,N*′-ethylenebis(2-aminomethyl-4-bromo-6-formylphenolato)copper(II) ([Cu(L′)]) with ethylenediamine; the main product obtained in this reaction is mononuclear [Cu(L)].[5] The complex $[Cu_2(R)]$ has the two Cu^{II} ions in the iminic sites and can accommodate two Ni^{II} ions in the vacant aminic sites, affording a mixed-metal $Cu^{II}_2Ni^{II}_2$ complex of a deficient double-cubane structure.[4] The macrocyclic ligand R^{4-} is differentiated from analogous macrocycles having four $N(imine)_2O_2$ or four $N(imine)_2O_2$ metal-binding sites[6] (Chart 1); the latter macrocyclic ligands with four equivalent metal-binding sites afford homonuclear metal com-

Scheme 1. Reaction of [Cu(L′)] with Ethylenediamine Providing the [1:1] and [2:2] Condensation Products

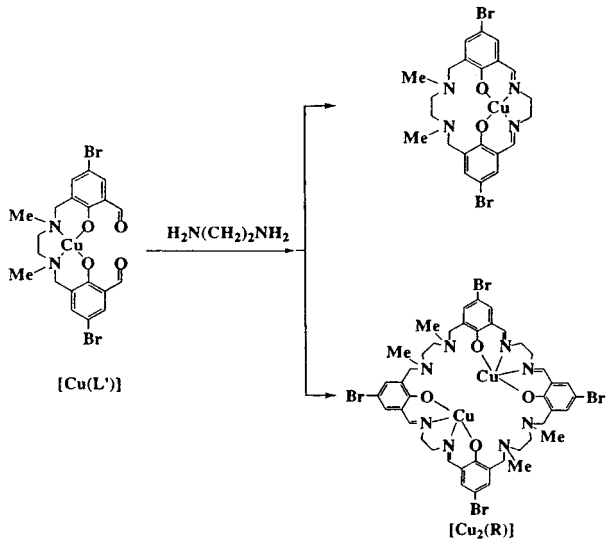

(1) Kahn, O. *Struct. Bonding* **1987**, *68*, 89.
(2) Murray, K. S. *Adv. Inorg. Chem.* **1995**, *42*, 261.
(3) Ōkawa, H.; Furutachi, H. Fenton, D. E. *Coord. Chem. Rev.* **1998**, *174*, 51.
(4) Yonemura, M.; Ōkawa, H.; Ohba, M.; Fenton, D. E.; Thompson, L. K. *J. Chem. Soc., Chem. Commun.* **2000**, 817.
(5) Yonemura, M.; Usuki, N.; Nakamura, Y.; Ōkawa, H. *J. Chem. Soc., Dalton Trans.*, in press.

10.1021/ic001162z CCC: $20.00
Published on Web 06/21/2001

Chart 1. Phenol-Based Tetranucleating Macrocycles with Four N(amine)$_2$O$_2$ Sites (left) and Four N(imine)$_2$O$_2$ Sites (Right)

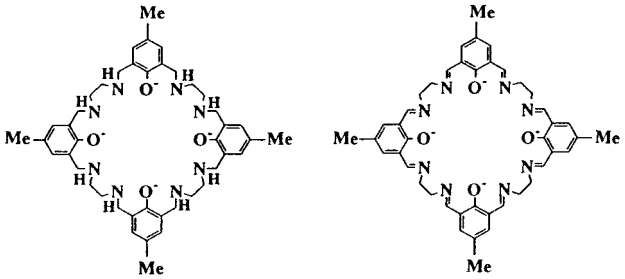

plexes. For further studies of mixed-metal Ma_2Mb_2 complexes using R^{4-}, establishing an efficient synthetic method of the macrocyclic ligand R^{4-} is desired.

In this work, the macrocylic ligand was prepared in a quantitative yield as $[Cu_2(H_2R)](ClO_4)_2$, by the reaction between [Cu(L′)] and ethylenediamine in the presence of perchloric acid. $[Cu_2(H_2R)](ClO_4)_2$ was converted into $[Cu_2(R)]$ by neutralization, and a series of mixed-metal complexes, $[Cu_2M_2(R)Cl_4]$ ($M = Co^{II}$ (**1**), Ni^{II} (**2**), Zn^{II} (**3**)), have been derived from $[Cu_2(R)]$. The structures and physicochemical properties of **1**−**3** are reported.

Experimental Section

Physical Measurements. Elemental analyses of carbon, hydrogen, and nitrogen were obtained at The Service Center for Elemental Analysis at Kyushu University. Metal analyses were made on a Shimadzu AA-680 atomic absorption/flame emission spectrophotometer. Infrared spectra were measured using a KBr disk with a Perkin-Elmer Spectrum BX FT-IR system. Fast atom bombardment (FAB) mass spectra were recorded on a JMS-SX/SX102A tandem mass spectrometer using *m*-nitrobenzyl alcohol as a matrix. Electronic absorption spectra in dimethyl sulfoxide (DMSO) were recorded on a Shimadzu UV-3100PC spectrophotometer. Reflectance spectra were recorded on the same spectrophotometer. Magnetic susceptibilities of powdered samples were measured on a Quantum Design MPMS XL SQUID susceptometer in the temperature range 2−300 K under an applied magnetic field of 500 G. Diamagnetic corrections were made with Pascal's constants.[7] Effective magnetic moments were calculated by the equation $\mu_{eff} = (8\chi_M T)^{1/2}$, where χ_M is the molar magnetic susceptibility corrected for diamagnetism of the constituting atoms.

Materials. All chemicals were purchased from commercial sources and used without further purification. TBAP was purified by recrystallization from ethanol and dried in vacuo.

Preparations. Synthesis of the proligand, *N*,*N*′-dimethyl-*N*,*N*′-ethylenedi(5-bromo-3-formyl-2-hydroxybenzylamine) (H_2L'), and its Cu^{II} complex [Cu(L′)] was reported previously.[8]

$[Cu_2(H_2R)](ClO_4)_2$. To a solution of ethylenediamine (ca. 10 cm^3) in DMF (ca. 10 cm^3) was added powdered [Cu(L′)] (1.15 g, 2.0 mmol), and the mixture was stirred for 2 h at room temperature. The resulting deep green suspension was acidified with an aqueous solution of perchloric acid (ca. 35%, ca. 20 cm^3) to give a brown precipitate. It was collected, washed with diethyl ether, and dried in vacuo. The yield was nearly quantitative based on [Cu(L′)]. Anal. Calcd for $C_{44}H_{50}Br_4Cl_2Cu_2N_8O_{12}$: C, 37.73; H, 3.60; N, 8.00; Cu, 9.07. Found: C, 37.70; H, 3.66; N, 7.86; Cu, 8.41. Selected IR data (ν/cm^{-1}): 1626 (s), 1445 (s), 1311 (m), 1100 (s), 624 (m). UV−vis (λ_{max}/nm (ϵ/mol^{-1} dm^3 cm^{-1})): 531 (718) in DMSO; 369 sh, 530 on a powdered sample. FAB-mass (*m*/*z*): 1301 for $\{[Cu_2(H_2R)]ClO_4\}^+$. Recrystallization from methanol formed $[Cu_2(H_2R)](ClO_4)_2 \cdot 2H_2O$ as good crystals suitable for X-ray crystallography.

$[Cu_2(R)]$. To a solution of $[Cu_2(H_2R)](ClO_4)_2$ (1.40 g, 1.00 mmol) in acetonitrile (ca. 30 cm^3) were added an acetonitrile solution (ca. 5 cm^3) of triethylamine (0.20 g, 1.98 mmol) and potassium carbonate (0.40 g, 2.90 mmol), and the mixture was stirred under reflux for 4 h to form a brown precipitate. It was collected by suction filtration, washed successively with water, and dried in vacuo. The yield was 0.81 g (67%). It was identified by comparing its IR spectrum with that of the authentic sample.[4] FAB-mass (*m*/*z*): 1199 for $\{Cu_2(R) + H\}^+$.

Cu_2M_2 Chloride Complexes (1−3). A solution of a hydrated metal(II) chloride (1.0 mmol) in methanol (10 cm^3) was added dropwise to a suspension of $[Cu_2(R)]$ (600 mg, 0.5 mmol) in acetonitrile (ca. 20 cm^3), and the mixture was stirred under reflux for 1 h. The resulting precipitate was collected by suction filtration, washed with diethyl ether, and dried in air.

$[Cu_2Co_2(R)Cl_4]\cdot 2H_2O$ (1) was obtained as a green crystalline powder. Yield: 87%. Anal. Calcd for $C_{44}H_{52}Br_4Cl_4Co_2Cu_2N_8O_6$: C, 35.34; H, 3.32; N, 7.68; Cu, 8.71; Co, 7.88. Found: C, 35.33; H, 3.33; N, 7.65; Cu, 8.62; Co, 7.87. Selected IR data (ν/cm^{-1}): 1631 (s), 1441 (s), 1288 (s). UV−vis (λ_{max}/nm): ∼380, ∼450, ∼580, ∼800 on a powdered sample. FAB-mass (*m*/*z*): 1423 for $\{Cu_2Co_2(R)Cl_3\}^+$.

A chloroform solution of **1** was diffused with methanol to form $[Cu_2Co_2(R)Cl_4]\cdot 2CHCl_3\cdot H_2O$ (**1′**) as large crystals suitable for X-ray crystallography.

$[Cu_2Ni_2(R)Cl_4]$ (2) was obtained as a brown crystalline powder. Yield: 50%. Anal. Calcd for $C_{44}H_{48}Br_4Cl_4Cu_2N_8Ni_2O_4$: C, 36.23; H, 3.32; N, 7.68; Cu, 8.71; Ni, 8.05. Found: C, 35.98; H, 3.32; N, 7.65; Cu, 8.62; Ni, 7.85. Selected IR data (ν/cm^{-1}): 1639 (s), 1438 (s), 1273 (m). UV−vis (λ_{max}/nm): ∼370, ∼460, 545, 800 nm on a powdered sample. FAB-mass (*m*/*z*): 1423 for $\{Cu_2Ni_2(R)Cl_3\}^+$.

$[Cu_2Zn_2(R)Cl_4]$ (3) was obtained as a green crystalline powder. Yield: 59%. Anal. Calcd for $C_{44}H_{48}Br_4Cl_4Cu_2N_8O_4Zn_2$: C, 35.90; H, 3.29; N, 7.61; Cu, 8.63; Zn, 8.88. Found: C, 35.80; H, 3.31; N, 7.57; Cu, 8.40; Zn, 8.94. Selected IR data (ν/cm^{-1}): 1633 (s), 1439 (s), 1290 (m). UV−vis (λ_{max}/nm): ∼380, ∼450, 580, 760 nm on powdered sample. FAB-mass (*m*/*z*): 1437 for $\{Cu_2Zn_2(R)Cl_3\}^+$.

A chloroform solution of **3** was layered with methanol to form large crystals of $[Cu_2Zn_2(R)Cl_4]\cdot 2CHCl_3\cdot H_2O$ (**3′**).

X-ray Crystallography for $[Cu_2(H_2R)](ClO_4)_2\cdot 2H_2O$, $[Cu_2Co_2(R)Cl_4]\cdot 2CHCl_3\cdot H_2O$ (1′), and $[Cu_2Zn_2(R)Cl_4]\cdot 2CHCl_3\cdot H_2O$ (3′). Crystallographic measurements were done on a Rigaku AFC7R diffractometer with graphitee-monochromated Mo Kα radiation ($\lambda = 0.710\,69$ Å) and a 12 kW rotating anode generator. Cell constants and an orientation matrix for the data collection were obtained from 25 reflections, and the $\omega-2\theta$ scan mode was used for intensity correction at 23 ± 1 °C. The octant measured was $+h,+k,\pm l$ for $[Cu_2(H_2R)](ClO_4)_2\cdot 2H_2O$, $+h,-k,\pm l$ for **1′**, and $\pm h,+k,\pm l$ for **3′**. Pertinent crystallographic parameters are summarized in Table 1.

Three standards were monitored every 150 measurements, and a linear correction factor was applied to the data to account for the decay phenomena obseved. Intensity data were corrected for Lorentz and polarization effects.

The structures were solved by direct methods and expanded using Fourier techniques. The non-hydrogen atoms were refined anisotropically. Because the chloroform molecules in **1′** and **3′** showed disorder, the refinements for the molecules were performed isotropically. All calculations were carried out on an IRIS Indy O_2 computer using the TEXSAN crystallographic software package.[9]

Results and Discussion

$[Cu_2(H_2R)](ClO_4)_2$ and $[Cu_2(R)]$. In the previous work[4] the reaction of stoichiometric amounts of [Cu(L′)] and ethylenediamine in DMF afforded the [1:1] condensation product [Cu(L^{2,2})] (see Scheme 1) along with a small amount of the [2:2]

(6) (a) Nanda, K. K.; Venkatsubramanian, K.; Majumdar, D.; Nag, K. *Inorg. Chem.* **1994**, *33*, 1581. (b) Nanda, K. K.; Mohanta, S.; Florke, U.; Dutta, S. K.; Nag, K. *J. Chem. Soc., Dalton Trans.* **1995**, 3831. (c) Mohanta, S.; Nanda, K. K.; Werner, R.; Haase, W.; Mukherjee, A. K.; Dutta, S. K.; Nag, K. *Inorg. Chem.* **1997**, *36*, 4656.
(7) *Landolt-Börnstein, Neue Series II/11*; Springer-Verlag: Berlin, 1981.
(8) Yonemura, M.; Matsumura, Y.; Ohba, M.; Okawa, H.; Fenton, D. E. *Chem. Lett.* **1996**, 601.
(9) TEXSAN, Molecular Structure Analysis Package; Molecular Structure Corp., Houston, TX, 1985 and 1992.

Table 1. Crystallographic Data of $[Cu_2(H_2R)](ClO_4)_2\cdot 2H_2O$, $[Cu_2Co_2(R)Cl_4]\cdot 2CHCl_3\cdot H_2O$ (1′) and $[Cu_2Zn_2(R)Cl_4]\cdot 2CHCl_3\cdot H_2O$ (3′)

	$[Cu_2(H_2R)](ClO_4)_2\cdot 2H_2O$	1′	3′
formula	$C_{44}H_{54}N_8Br_4Cl_2Cu_2O_{14}$	$C_{46}H_{52}N_8Br_4Cl_{10}Co_2Cu_2O_5$	$C_{46}H_{52}N_8Br_4Cl_{10}Zn_2Cu_2O_5$
fw	1436.57	1716.08	1728.96
cryst syst	monoclinic	monoclinic	monoclinic
space group	$P2_1/c$ (No. 14)	$C2/c$ (No. 15)	$C2/c$ (No. 15)
a/Å	19.603(3)	32.514(3)	32.53(1)
b/Å	13.370(2)	12.246(3)	12.242(2)
c/Å	21.072(3)	19.827(2)	19.729(9)
β/deg	98.87(1)	126.082(5)	126.03(3)
V/Å^3	5456(1)	6380(1)	6354(4)
Z	4	4	4
temp/°C	23 ± 1	23 ± 1	23 ± 1
ρ_{calcd}/g cm^{-3}	1.748	1.786	1.807
μ(Mo Kα)/cm^{-1}	38.84	41.48	43.97
no. of observns (all data)	10 147	6921	5895
R^a ($I > 2\sigma(I)$)	0.053	0.066	0.062
$R_w{}^b$	0.186	0.204	0.198

^{a} $R = \sum||F_o| - |F_c||/\sum|F_o|$. ^{b} $R_w = [\sum w(F_o^2 - F_c^2)^2/\sum w(F_o^2)^2]^{1/2}$, $w = 1/[\sigma^2(F_o^2)]$.

Scheme 2 Proposed Synthetic Mechanism for $[Cu_2(H_2R)](ClO_4)_2$

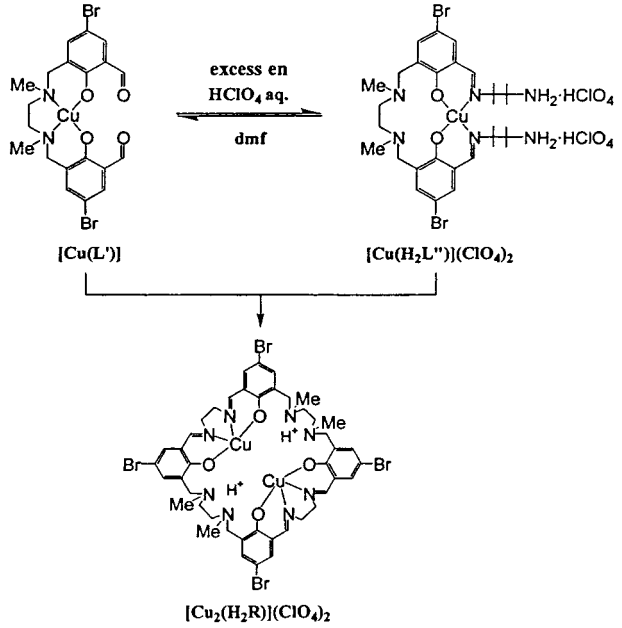

condensation product $[Cu_2(R)]$.[4] In the present work, the reaction of [Cu(L′)] with a large excess of ethylenediamine under acidic conditions with perchloric acid gave the [2:2] condensation product $[Cu_2(H_2R)](ClO_4)_2$ in a quantitative yield. Such acidic conditions have often been used for nontemplate cyclization reactions.[10,11] The reaction of [Cu(L′)] with ethylenediamine under acidic conditions may result in the acyclic Schiff base complex $[Cu(H_2L'')](ClO_4)_2$, which is in equilibrium with [Cu(L′)] in the solution (Scheme 2). The [1:1] condensation between [Cu(L′)] and $[Cu(H_2L'')](ClO_4)_2$, followed by the rearrangement of the metal ions, leads to the formation of $[Cu_2(H_2R)](ClO_4)_2$.

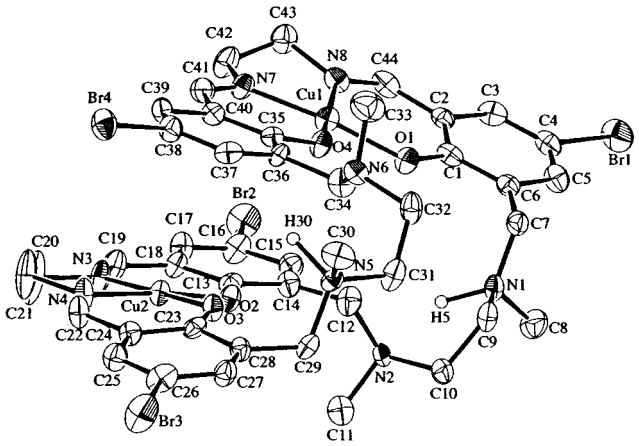

Figure 1. ORTEP view of $[Cu_2(H_2R)](ClO_4)_2\cdot 2H_2O$ with the atom-numbering scheme.

Table 2. Selected Bond Distances and Angles of $[Cu_2(H_2R)](ClO_4)_2\cdot 2H_2O$

Bond Distances (Å)			
Cu(1)−O(1)	1.905(6)	Cu(1)−O(4)	1.878(6)
Cu(1)−N(7)	1.925(7)	Cu(1)−N(8)	1.936(8)
Cu(2)−O(2)	1.909(6)	Cu(2)−O(3)	1.922(6)
Cu(2)−N(3)	1.921(8)	Cu(2)−N(4)	1.937(8)
N(1)···N(2)	2.840(11)	N(5)···N(6)	2.756(11)
Cu(1)···Cu(2)	6.533(2)		
Bond Angles (deg)			
O(1)−Cu(1)−O(4)	88.4(3)	O(1)−Cu(1)−N(7)	172.1(3)
O(1)−Cu(1)−N(8)	93.9(3)	O(4)−Cu(1)−N(7)	94.6(3)
O(4)−Cu(1)−N(8)	170.1(3)	N(7)−Cu(1)−N(8)	84.3(3)
O(2)−Cu(2)−O(3)	92.2(3)	O(2)−Cu(2)−N(3)	92.8(3)
O(2)−Cu(2)−N(4)	173.4(3)	O(3)−Cu(2)−N(3)	174.9(3)
O(3)−Cu(2)−N(4)	92.2(3)	N(3)−Cu(2)−N(4)	82.9(4)

The structure of $[Cu_2(H_2R)](ClO_4)_2\cdot 2H_2O$ has been determined by the single-crystal X-ray method. An ORTEP[12] view is given in Figure 1, and selected bond distances and angles are given in Table 2. Two Cu^{II} ions reside in the iminic sites of the macrocyclic ligand, affording a $\{CuN_2O_2\}$ chromophore similar to that of [Cu(salen)].[13] Two protons exist in the two aminic sites and are hydrogen-bonded between the two amine nitrogens (N1- - -H5- - -N2 and N5- - -H30- - -N6): the N1- - -N2 and N5- - -N6 separations are 2.840(11) and 2.756(11) Å, respectively. Because of these hydrogen bonds, the complex molecule assumes a U shape with a near-parallel arrangement of the two $\{CuN_2O_2\}$ moieties. Two $\{CuN_2O_2\}$ chromophores form a dihedral angle of 157.0°.

The FAB mass spectrum of $[Cu_2(H_2R)](ClO_4)_2$ has an ion peak at m/z 1301 that corresponds to $\{Cu_2(H_2R)ClO_4\}^+$. The molar conductance in acetonitrile is 250 S cm^2 mol^{-1}, which is common for 2:1 electrolytes in this solvent.[14] The visible spectrum in DMSO has a d−d band maximum at 531 nm, in accord with a $\{CuN(imine)_2O_2\}$ chromophore similar to [Cu(salen)].[8,15] $[Cu_2(H_2R)](ClO_4)_2$ is converted into $[Cu_2(R)]$ by neutralization. The positive-ion FAB mass spectrum of $[Cu_2(R)]$ showed an ion peak at m/z 1199 that corresponds to $\{Cu_2(R) + H\}^+$.

$Cu^{II}_2M^{II}_2$ Complexes. General Characterization. The mixed-metal $Cu^{II}M^{II}$ complexes were readily prepared by the reaction of $[Cu_2(R)]$ with a M^{II} chloride salt in acetonitrile. Elemental

(10) Atkins, A. J.; Black, D.; Blake, J.; Marin-Becerra, A.; Parsons, S.; Ruiz-Ramirez, L.; Schröder, M. *J. Chem. Soc., Chem. Commun.* **1996**, 457.
(11) (a) Truex, T. J.; Holm, R. H. *J. Am. Chem. Soc.* **1971**, *93*, 285. (b) Truex, T. J.; Holm, R. H. *J. Am. Chem. Soc.* **1972**, *94*, 4529.
(12) Johnson, C. K. Report 3794; Oak Ridge National Laboratory, Oak Ridge, TN, 1965.
(13) Baker, E. N.; Hall, D.; Waters, T. N. *J. Chem. Soc. A* **1970**, 406.
(14) Geary, W. J. *Coord. Chem. Rev.* **1971**, *7*, 81.
(15) Ferguson, J. *J. Chem. Phys.* **1961**, *34*, 2206.

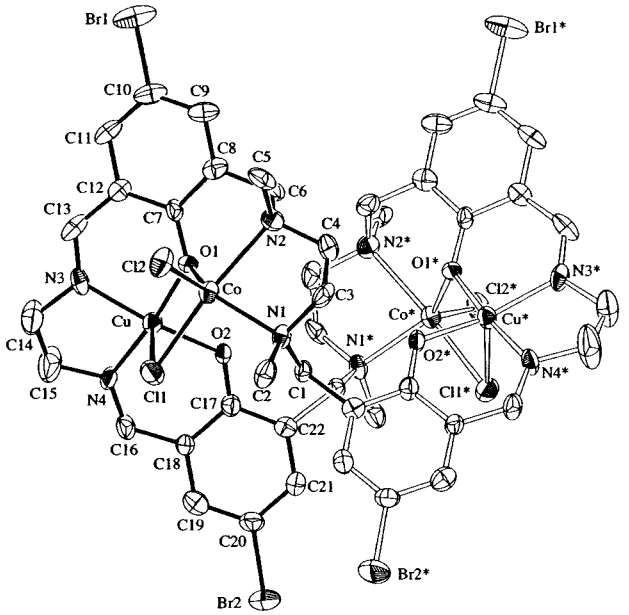

Figure 2. ORTEP view of $[Cu_2Co_2(R)Cl_4]\cdot 2CHCl_3\cdot H_2O$ (**1′**) with the atom-numbering scheme.

analyses of the products agreed well with the formula $Cu_2M_2(R)Cl_4(H_2O)_n$ ($n = 2$ for Co^{II} (**1**); $n = 0$ for Ni^{II} (**2**) and Zn^{II} (**3**)). The FAB mass spectra of **1**−**3** have an ion peak corresponding to $\{CuM(R)Cl_3\}^+$. No ion peak due to Cu_4 and M_4 species was recognized in the FAB mass spectra, indicating a discrete mixed-metal core of these complexes.

Crystal Structures. The two complexes $[Cu_2Co_2(R)Cl_4]\cdot 2CHCl_3\cdot H_2O$ (**1′**) and $[Cu_2Zn_2(R)Cl_4]\cdot 2CHCl_3\cdot H_2O$ (**3′**) are isostructural. The crystal structure of **1′** is discussed here. An ORTEP view of the essential part of **1′** is shown in Figure 2 together with the atom-numbering scheme. Selected bond distances and angles of **1′** and **3′** are summarized in Table 3.

The asymmetric unit of **1′** consists of half of the macrocycle (R),$^{4-}$ one Cu^{II} ion, one Co^{II} ion, and four chloride ions. Two chloroform molecules and one water molecule are free from coordination and are captured in the crystal lattice. Each Cu^{II} ion resides in the iminic site and has a five-coordinate geometry with a chloride ion at the apical position; the chloride ion is involved in the bridge to the adjacent Co^{II}. The discrimination parameter τ[16] between a square pyramid ($\tau = 0$) and a trigonal bipyramid ($\tau = 1$) is 0.193 for the Cu. The displacement of the Cu from the basal N_2O_2 least-squares plane toward the apical Cl is 0.123 Å. The equatorial Cu-to-ligand bond distances range from 1.902(9) to 1.97(1) Å. The axial Cu−Cl bond distance is 2.674(3) Å, which is elongated due to the Jahn−Teller effect in the d^9 electronic configration.

The Co^{II} forms bonds to the phenolic oxygen O1, the amino nitrogens N1 and N2, the bridging chloride ion Cl(1), and the terminal chloride ion Cl(2). The geometry about the metal ion is intermediate between a square pyramid and a trigonal bipyramid, as determined from the τ value of 0.583. The Co−Cl(1) bond distance in the bridge (2.383(3) Å) is long relative to the terminal Co−Cl(2) distance (2.308(3) Å). The Cu- - -Co interatomic separation, bridged by the phenolic oxygen O1 and the chloride ion Cl(1), is 3.272(2) Å.

The two CuCo units in the molecule are separated from one another, providing a dimer-of-dimers structure. The intermetallic Cu- - -Co*, Cu- - -Cu* and Co- - -Co* separations are 6.847(2), 8.000(2), and 7.119(3) Å, respectively (symmetry operation (*): $-x, y, -z - {}^1/_2$).

Table 3. Selected Bond Distances and Angles of 1′ and 3′[a]

	M = Co (**1′**)	Zn (**3′**)
	Bond Distances (Å)	
Cu−O(1)	1.946(6)	1.949(5)
Cu−O(2)	1.928(7)	1.926(6)
Cu−N(3)	1.97(1)	1.959(8)
Cu−N(4)	1.902(9)	1.929(8)
Cu−Cl(1)	2.674(3)	2.675(3)
M−O(1)	2.040(7)	2.090(6)
M−N(1)	2.125(8)	2.140(7)
M−N(2)	2.285(9)	2.331(7)
M−Cl(1)	2.383(3)	2.402(3)
M−Cl(2)	2.308(3)	2.288(3)
Cu···M	3.272(2)	3.334(3)
Cu···Cu*	8.000(2)	7.992(5)
Cu···M*	6.847(2)	6.898(4)
M···M*	7.119(3)	7.270(4)
	Bond Angles (deg)	
Cl(1)−Cu−O(1)	80.7(2)	80.7(2)
Cl(1)−Cu−O(2)	96.2(2)	97.6(2)
Cl(1)−Cu−N(3)	102.1(3)	101.5(3)
Cl(1)−Cu−N(4)	96.5(3)	95.3(3)
O(1)−Cu−O(2)	94.4(3)	94.8(2)
O(1)−Cu−N(3)	90.1(3)	90.8(3)
O(1)−Cu−N(4)	173.0(4)	172.5(3)
O(2)−Cu−N(3)	161.6(3)	160.7(3)
O(2)−Cu−N(4)	92.3(3)	92.0(3)
N(3)−Cu−N(4)	84.2(4)	83.8(3)
Cl(1)−M−Cl(2)	98.2(1)	99.8(1)
Cl(1)−M−O(2)	86.6(2)	85.0(2)
Cl(1)−M−N(1)	96.9(2)	95.3(2)
Cl(1)−M−N(2)	165.8(2)	162.3(2)
Cl(2)−M−O(1)	121.0(2)	121.9(2)
Cl(2)−M−N(1)	107.1(2)	109.1(2)
Cl(2)−M−N(2)	95.7(2)	97.6(2)
O(1)−M−N(1)	130.8(3)	128.2(3)
O(1)−M−N(2)	83.8(3)	83.1(2)
N(1)−M−N(2)	81.7(3)	81.9(3)
Cu−Cl(1)−M	80.49(9)	81.87(8)
Cu−O(1)−M	110.4(3)	111.2(3)

[a] Symmetry operation (*): $-x, y, -{}^1/_2 - z$.

In the isostructural **3′**, the discriminating parameter (τ) for Zn^{II} is 0.568 and the Cu- - -Zn separation is 3.333(3). The intermetallic Cu- - -Zn*, Cu- - -Cu* and Zn- - -Zn* separations are 6.899(4), 7.993(5), and 7.271(4) Å, respectively.

The structure of $[Cu_2Ni_2(R)Cl_2]Cl_2\cdot H_2O$ (**2′**) was preliminarily reported.[4] This complex has a defect double-cubane structure (Figure 3). Each Cu^{II} resides in the iminic site and assumes a square-pyramidal geometry with further coordination of a chloride ion at the axial site. Each Ni^{II} resides in the aminic site and assumes a pseudo-octahedral geometry together with two chloride ions in cis positions. One phenolic oxygen (O1) of one $\{CuN_2O_2\}$ unit forms a bond to Ni*, and another phenolic oxygen (O2) forms a bond to Ni. The Cl(1) acts as a μ_3 bridge to Cu, Ni, and Ni*, and the Cl(1*) acts as a μ_3 bridge to Cu*, Ni, and Ni* (symmetry operation (*): $-x, y, -z$). The geometry about each Ni is pseudo-octahedral. The Cu- - -Ni, Cu- - -Ni*, Ni- - -Ni*, and Cu- - -Cu* separations in the defect double cubane are 3.376(2), 3.365(2), 3.540(2), and 5.736(3) Å, respectively. The remaining two chloride ions are not involved in coordination and are captured in the crystal lattice.

Thus **1** and **3** have a dimer-of-dimers structure, whereas **2** has a defect double-cubane structure. The different core structures arise from the geometrical preference of the M^{II} ion. Co^{II} and Zn^{II} in **1′** and **3′** can assume a distorted five-coordinate

(16) Addison, A. W.; Rao, T. N.; Reedijk, J.; Rijn, J. V.; Verschoor, G. C. *J. Chem. Soc., Dalton Trans.* **1984**, 1349.

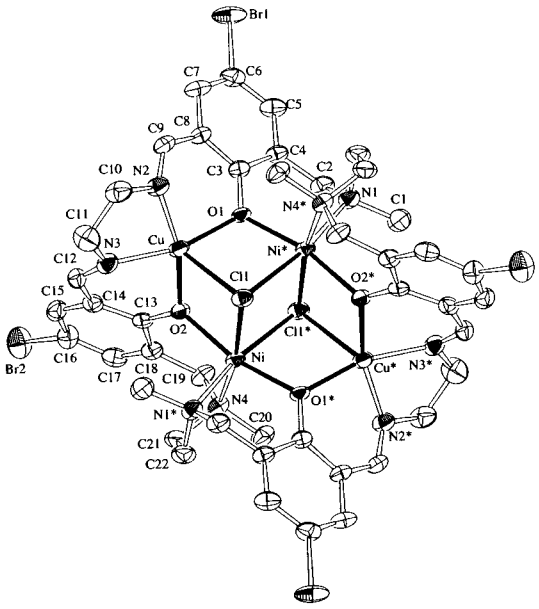

Figure 3. ORTEP view of $[Cu_2Ni_2(R)Cl_4]$ (**2**) with the atom-numbering scheme.

geometry, whereas Ni^{II} in **2′** prefers octahedral six-coordination to a distorted five-coordinate geometry.

Electronic Spectra. Complexes were insoluble in most organic and inorganic solvents. The electronic spectra for **1**−**3** were measured on powdered samples. All the complexes show four bands at ∼380, ∼460, ∼570, and ∼780 nm. The intense band at ∼380 nm is assigned to the $\pi-\pi^*$ transition associated with the azomethine group.[17,18] The discernible shoulder near 450 nm can be assigned to the Cl^--to-Cu^{II} charge-transfer band[19] and the two visible bands to the d−d components of the Cu ion. The spectral feature is in accord with the involvement of the chloride ion in the coordination to Cu^{II}, providing a square-pyramidal $\{Cu^{II}N_2O_2Cl\}$ chromophore. The d−d bands due to the M^{II} ion are not resolved for **1** and **2** because high-spin Co^{II} and Ni^{II} generally show weak d−d transition bands.

Magnetic Properties. The magnetic properties of **3** with a dimer-of-dimers structure is first discussed because this is the simplest case among the present complexes. It has a magnetic moment of 1.81 μ_B (per Cu) at room temperature, and the moment was practically independent of temperature down to 2 K (1.79 μ_B). Evidently, the magnetic interaction between the two CuZn units in a molecule is negligibly weak.

The μ_{eff} vs T and χ_M vs T curves of **1** (per CuCo) are given in Figure 4. The effective magnetic moment is 4.77 μ_B at room temperature, and the moment decreased with decreasing temperature to 1.96 μ_B at 2 K. On the basis of the magnetic nature of **3** discussed above, magnetic analyses for **1** have been done by considering the magnetic interaction within the dinuclear Co^{II}-Cu^{II} unit. On the basis of the Heisenberg Hamiltonian ($H = -2JS_{Cu}S_{Co}$),[20] the magnetic susceptibility equation for Cu^{II}($S = {}^1/_2$)−Co^{II}($S = {}^3/_2$) is given by eq 1,[21] where χ_M is the magnetic

$$\chi_M = \{2N\beta^2/k(T-\Theta)\}[10g_2^2 + 2g_1^2\exp(-4J/kT)]/[5 + 3\exp(-4J/kT)] + N\alpha \quad (1)$$

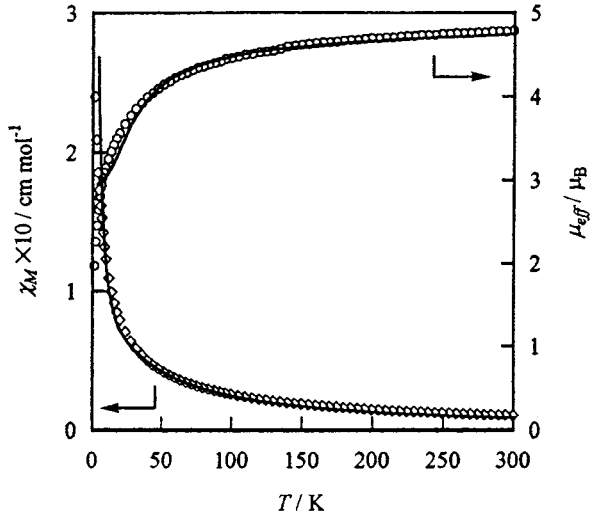

Figure 4. χ_M vs T and μ_{eff} vs T curves for $[Cu_2Co_2(R)Cl_4]$ (**1**).

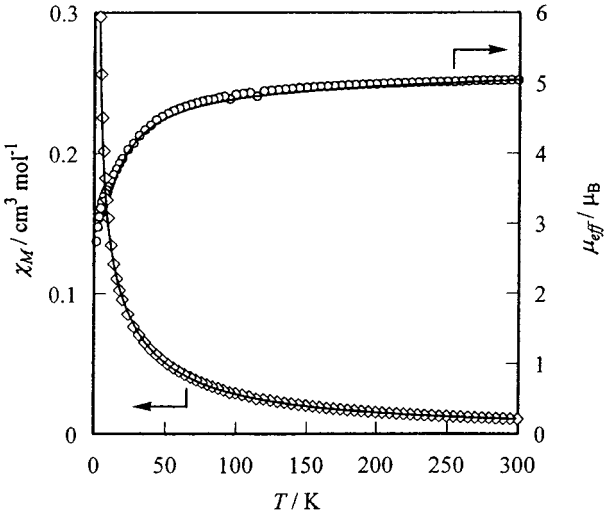

Figure 5. χ_M vs T and μ_{eff} vs T curves for $[Cu_2Ni_2(R)Cl_4]$ (**2**).

susceptibility per CuCo, N is Avogadro's number, β is the Bohr magneton, k is the Boltzmann constant, T is the abosolute temperature, J is the exchange integral, and $N\alpha$ is the temperature-independent paramagnetism. The Weiss constant Θ is introduced as the correction term for secondary contributions. The g_1 and g_2 values are the g factors associated with the total spin states $S_T = 1$ and $S_T = 2$, respectively, and are expressed using local g_{Cu} and g_{Co} factors such as $g_1 = (5g_{Co} - g_{Cu})/4$ and $g_2 = (3g_{Co} + g_{Cu})/4$.[1,22,23] A good best-fit is obtained as shown by the solid line in Figure 4, using $J = -9.5$ cm^{-1}, $g_{Cu} = 2.10$, $g_{Co} = 2.23$, $\Theta = -0.5$ K, and $N\alpha = 300 \times 10^{-6}$ cm^3 mol^{-1}. The discrepancy factor defined as $R(\mu) = [\sum(\mu_{obsd} - \mu_{calcd})^2/\sum(\mu_{obsd})^2]^{1/2}$ was 3.58×10^{-2}.

The μ_{eff} vs T and χ_M vs T curves of **2** (per Cu_2Ni_2) are given in Figure 5. The effective magnetic moment at room temperature is 5.03 μ_B, which decreased with decreasing temperature to 2.72 μ_B at 2 K. On the basis of the crystallographic result in Figure 3, the spin system with four equivalent Cu−Ni interactions (exchange integral: J) and one Ni−Ni interaction (J') is

(17) Bosnich, B. *J. Am. Chem. Soc.* **1968**, *90*, 627.
(18) Downing, R. S.; Urbach, F. L. *J. Am. Chem. Soc.* **1969**, *91*, 5977.
(19) Yonemura, M.; Ohba, M.; Takahashi, K.; Okawa, H.; Fenton, D. E. *Inorg. Chim. Acta* **1998**, *283*, 72.
(20) Heisenberg, W. *Z. Phys.* **1926**, *38*, 411.
(21) Okawa, H.; Nishio, J.; Ohba, M.; Tadokoro, M.; Matsumoto, N.; Koikawa, M.; Kida, H.; Fenton, D. E. *Inorg. Chem.* **1993**, *32*, 2949.
(22) Chao, C. C. *J. Magn. Reson.* **1973**, *10*, 1.
(23) Scarlinge, R. P.; Hodgson, D. J.; Hatfield, W. E. *Mol. Phys.* **1978**, *35*, 701.

Chart 2. Spin System for $[Cu_2Ni_2(R)Cl_4]$ (**3**)

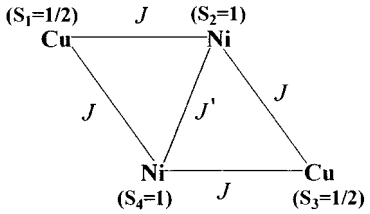

considered (Chart 2); the magnetic interaction between Cu^1 and Cu^3 can be neglected because of the large Cu- - -Cu* separation (5.735 Å). Using the spin Hamiltonian $H = -2J(S_1 \cdot S_2 + S_2 \cdot S_3 + S_3 \cdot S_4 + S_1 \cdot S_4) - 2J'S_2 \cdot S_4$, the magnetic susceptibility expression for the system is derived as

$$\chi_M = (2Ng^2\beta^2/kT)\{A/B\} \qquad (2)$$

with $A = 14 \exp[(4J + 6J')/kT] + 5 \exp[(-2J + 6J')/kT] + \exp[(-6J + 6J')/kT] + 5 \exp[(2J + 2J')/kT] + \exp[(-2J + 2J')] + 5 \exp(6J'/kT) + \exp(2J'/kT) + 1$ and $B = 7 \exp[(4J + 6J')/kT] + 5 \exp[(-2J + 6J')/kT] + 3 \exp[(-6J + 6J')/kT] + 5 \exp[(2J + 2J')/kT] + 3 \exp[(-2J + 2J')/kT] + \exp[(-4J + 2J')/kT] + 5 \exp(6J'/kT) + 3 \exp(2J'/kT) + 4$.

A good magnetic simulation is obtained with eq 2, as shown in Figure 5, using the parameters $J = -3.5\ cm^{-1}$, $J' = +2.0\ cm^{-1}$, $g = 2.14$, $\Theta = -0.5$ K, and $N\alpha = 560 \times 10^{-6}\ cm^3\ mol^{-1}$. The discrepancy factor $R(\mu)$ was 1.13×10^{-2}. The result indicates a weak antiferromagnetic interaction between the adjacent Cu^{II} and Ni^{II} centers and a weak ferromagnetic interaction between the two Ni^{II} centers.

Conclusions

An efficient synthetic method for the tetranucleating macrocyclic ligand R^{4-} has been established, and the mixed-metal $Cu^{II}{}_2M^{II}{}_2$ complexes $[Cu_2M_2(R)Cl_4]$ ($M = Co^{II}$ (**1**), Ni^{II} (**2**), Zn^{II} (**3**)) have been derived. X-ray crystallographic studies indicate that **1** and **3** have a dimer-of-dimers structure, whereas **2** has a defect double-cubane structure. In the dimer-of-dimers structure of **1** and **3**, the M^{II} ion assumes a distorted five-coordination. In the defect double-cubane structure of **2**, the Ni^{II} has an octahedral geometry. Studies on $M_2M'_2$ complexes of R^{4-} in different combinations of metal ions are under way.

Acknowledgment. This work was supported by a Grant-in-Aid for Scientific Research on Priority Area "Metal-assembled Complexes" (No. 10149106) and a Grant-in-Aid for COE Research "Design and Control of Advanced Molecular Assembly System" (No. 08CE2005) from the Ministry of Education, Science, and Culture of Japan.

Supporting Information Available: Positional and thermal parameters of non-hydrogen atoms and all bond distances and angles for $[Cu_2(H_2R)](ClO_4)_2 \cdot 2H_2O$, $[Cu_2Co_2(R)Cl_4] \cdot 2CHCl_3 \cdot H_2O$ (**1′**), and $[Cu_2Zn_2(R)Cl_4] \cdot 2CHCl_3 \cdot H_2O$ (**3′**) in CIF format. This material is available free of charge via the Internet at http://pubs.acs.org.

IC001162Z